POLITECNICO DI TORINO
Repository ISTITUZIONALE

A machine learning tool for future prediction of heat release capacity of in-situ flame retardant hybrid Mg(OH)2-Epoxy nanocomposites

(Article begins on next page)

A machine learning tool for future prediction of heat release capacity of in-situ flame retardant hybrid Mg(OH)$_2$-Epoxy nanocomposites

Aurelio Bifulco [a], Angelo Casciello [a], Claudio Imparato [a], Stanislao Forte [b], Sabyasachi Gaan [c], Antonio Aronne [a], Giulio Malucelli [d,*]

[a] Department of Chemical Materials and Production Engineering (DICMaPI), University of Naples Federico II, Piazzale V. Tecchio 80, 80125, Naples, Italy
[b] Software Care Srl, Via Servio Tullio, 106, 80126, Naples, Italy
[c] Laboratory for Advanced Fibers, Empa Swiss Federal Laboratories for Materials Science and Technology, Lerchenfeldstrasse 5, 9014, St. Gallen, Switzerland
[d] Department of Applied Science and Technology, Politecnico di Torino, Viale Teresa Michel 5, Alessandria, 15121, Italy

ARTICLE INFO

ABSTRACT

In this work, the fire behavior of a sol-gel in-situ hybrid Mg(OH)$_2$-epoxy nanocomposite was investigated and an artificial neural network-based system built on a fully connected feed-forward artificial neural network was developed to predict its heat release capacity. The nanocomposite containing only ~5 wt% loading of Mg(OH)$_2$ promoted a remarkable decrease in heat release capacity (~34%) measured by pyrolysis combustion flow calorimetry and in peak of heat release rate (~37%), and heat release rate (~29%), as assessed by cone calorimetry, as well as a significant decrease of total smoke release and smoke extinction area about 22 and 5%, respectively, indicating the suitability of Mg(OH)$_2$ as an effective smoke suppressant. The proposed machine learning approach may be used as a promising alternative for a cost- and time-saving prediction of the fire performances of novel flame retardant polymer-based nanocomposites.

1. Introduction

Epoxy resins are widely used in several industrial applications, due to their peculiar properties in terms of thermal stability and chemical resistance [1,2]. Nevertheless, epoxy resins need the addition of suitable flame retardants to fulfill specific standards in the aerospace and automotive industry. The flame retardancy of epoxy resin can be enhanced by either the chemical modification of the polymer matrix, or the curing agent introducing functional moieties [3–5]. In this context, it is well known that metal hydroxides represent sustainable flame retardants able to work in the condensed phase. Metal hydroxides lower the heat transfer by endothermic decomposition and convert into refractive metal oxides acting as thermal shield and oxygen barrier during the combustion [6,7]. Among the available metal hydroxides, magnesium hydroxide (Mg(OH)$_2$) has shown good potentialities for improving the fire behavior of epoxy resins [8,9]. To be effective, large amounts (7–20 wt%) of Mg(OH)$_2$ are usually required [10–12], which represents a significant downside in terms of costs and mechanical properties of the final products. Recently, an in-situ sol-gel synthesis route was designed to obtain Mg(OH)$_2$ nanocrystals (at about 5 wt% loading) in a bisphenol

A diglycidyl ether (DGEBA)-based epoxy resin via an eco-friendly solvent-free one-pot process [13]. This methodology allows for the generation of finely and well-distributed nanocrystals, embedded in an organic-inorganic (hybrid) network, able to increase the thermal stability of epoxy, leading to the formation of an abundant and quite stable char in inert atmosphere [13,14]. By this strategy, in-situ hybrid epoxy nanocomposites showing good fire behavior can be prepared, even with low nanofiller loadings.

The development of new functional polymer-based materials with excellent fire performances often demands the investigation of several compositions by means of destructive tests. The possibility to predict the results of small-scale combustion tests (e.g. pyrolysis combustion flow calorimetry, PCFC) based on several physical and chemical properties of polymers would contribute to reduce the research efforts, especially during the design of a new material. In the literature, many research groups have used publicly available data about polymer properties to predict or optimize new polymer properties and fire parameters. For example, the molar group contribution method can predict the flammability parameters of many polymers [15,16]. However, this method is error-prone, due to the arbitrary assignment of chemical groups, and

* Corresponding author.
E-mail address: giulio.malucelli@polito.it (G. Malucelli).

shows strong limitations in the case of new materials, for which molar contributions are not available [17,18]. Machine learning allows for overcoming the limits linked to arbitrary assignments or human failures, as it uses algorithms or computational methods to learn information directly from data without relying on a predetermined equation as a model [19–21]. Artificial neural network models involve the application of different types of algorithms on input data [22]. Among them, a locally weighted regression algorithm is a non-parametric regression technique used to fit a surface or curve to a set of data points. Global regression models assume a single relationship between the response variable and the predictors, while local regression ones adapt to the local behavior of the data, allowing for more flexible and localized modeling. The local regression model fits a regression function to a subset of the data for each target point in the dataset. The subset consists of data points within the bandwidth of the target point. The weights assigned to each data point in this subset depend on their proximity to the target point, determined by the kernel function [23]. Overall, the local regression model gives more importance to nearby data points while downweighting or ignoring distant points: therefore, it adapts to the local patterns in the data. Thanks to that, the model can consider even complex relationships that may vary across different regions of the predictor space. Local regression is extremely useful when dealing with nonlinear relationships or when the underlying relationship between the predictors and the response variable is expected to vary across different regions of the data. Local regression provides a flexible and data-driven approach to modeling that can capture local behaviors and improve prediction accuracy [24]. Machine learning enables the prediction of fire performances related to new products and allows for assessing their suitability for a specific application [25,26]. Despite the potential of machine learning, overfitting can limit the accuracy of neural network models in predicting flammability parameters. The overfitting usually occurs when a model is extremely reliable on training data, but it fails when applied to never seen (i.e., not used for training the model) data. There are several approaches to control the overfitting and improve the accuracy of neural network models, for example increasing the size of the training dataset, applying early stopping, employing cross-validation, or simplifying the model architecture [27,28]. Parandekar et al. predicted the heat release capacity (HRC), the amount of char residue, and the total heat release (THR) of a set of different polymers using genetic function algorithms [29]. In particular, they correlated the flammability of the polymer to its chemical structure by quantitative structure–property relationships methodology, finding a good correlation between the polymer repeat unit structure and the flammability parameters [29]. Lately, Asante-Okyere et al. proposed a generalized regression neural network and a supervised learning algorithm-based feed-forward back propagation neural network to predict PCFC results, such as HRC, THR, peak of the heat release rate, heat release time, and related temperatures of polymethyl methacrylate using such parameters as heating rate and sample mass [30]. Both neural network models gave high correlation coefficients, despite some differences in the performances during training or testing according to the target value. With a similar approach and starting from the same input data, Mensah et al. predicted PCFC results of extruded polystyrene using feed-forward back-propagation neural networks and the group method of data handling [31]. The comparison of the HRC and heat of combustion prediction revealed an excellent accuracy and repeatability of the latter method, with a mean deviation of about 4. Recently, Pomázi and Toldy developed an artificial neural network-based system to predict the THR, the peak of the heat release, the time to ignition, and the char residue from structural properties and results from flammability tests (i.e. limiting oxygen index and UL-94 vertical burning test) [27]. The average absolute deviation between predicted and validated data was below 10% in most cases. They also carried out a sensitivity analysis of the output parameters in order to rank the input parameters based on their impact on the output parameters [27].

In this work, for the first time, the fire behavior and glass transition

temperature of epoxy nanocomposite containing $Mg(OH)_2$ nanocrystals, in-situ generated by sol-gel at mild operative conditions, without any use of surfactants and following a one-pot procedure, were investigated. The fire performances were evaluated by means of forced-combustion tests and pyrolysis combustion flow calorimetry measurements to collect the main parameters (e.g., HRC, THR, char residue) and shed light on the flame retardant action of $Mg(OH)_2$ nanocrystals during the combustion of the nanocomposite. Also, an artificial neural network-based system was developed to predict the HRC value of the prepared in-situ hybrid $Mg(OH)_2$-epoxy nanocomposite from the physico-chemical properties of polymers and their PCFC parameters. A machine learning approach was used to estimate the HRC of a novel material and a sensitivity analysis was performed to prove the accuracy of the implemented algorithm. Finally, the cross-validation method was employed during the hyperparameter tuning phase (with the "X-Partitioner" node) to avoid overfitting and find the best hyperparameters for each subset of the input data.

2. Materials and methods

2.1. Materials

Tetraethyl orthosilicate (TEOS, >99%), magnesium ethoxide (>98%), ethanol (ACS reagent, anhydrous) and 3-aminopropyl-triethoxysilane (APTS, >98%) were purchased from Sigma-Aldrich (Switzerland). To prepare composite laminates, a two-component epoxy resin system (SX10 by MATES S.r.l., Milan, Italy), consisting of bisphenol A diglycidyl ether (DGEBA) and modified cycloaliphatic polyamines, were employed.

2.2. Synthesis of Epoxy/Mg(OH)$_2$ nanocomposite

The in-situ synthesis of the hybrid $Mg(OH)_2$-epoxy nanocomposite was performed according to the procedure elsewhere reported [13], for which the main steps are briefly displayed in Fig. 1: (i) 20 g of DGEBA and 5.9 g of magnesium ethoxide were mixed overnight at 80 °C; (ii) 20 g of DGEBA and 3.5 g of APTS were stirred at 80 °C for 2 h, then this mixture was added, under stirring, to the first one at 80 °C for 30 min; (iii) ethanol (1.12 mL), distilled water (3.37 mL), and TEOS (TEOS/APTES molar ratio as low as 1.25) were added to the main batch at 80 °C under reflux for 90 min. Finally, the reaction vessel was opened and left at 80 °C for 30 min to completely remove water and ethanol. At room temperature, ~10.4 g of hardener was added to the mixture and mixed for 5 min. Before pouring into a Teflon mold, the resulting mixtures underwent degassing under vacuum. Samples were cured at 30 °C for 24 h, then post-cured at 80 °C for 4 h. The loading of magnesium hydroxide was evaluated from the stoichiometry around 5.2 wt%.

Using this procedure [32–34], both twinned $Mg(OH)_2$ nanocrystals with a pseudo-hexagonal symmetry and multisheet-silica nanoparticles were obtained in the epoxy matrix (Fig. 1) [13].

The in-situ hybrid $Mg(OH)_2$-epoxy nanocomposite will be coded as EPO-Mg throughout the whole text, while the acronym EPO will be used for the unmodified epoxy resin.

2.3. Characterization

Differential scanning calorimetry (DSC) measurements were performed under a N_2 flow (50 mL/min) using a DSC 214 Polyma instrument (NETZSCH-Gerätebau GmbH, Selb, Germany). The measurements were carried out according to the following cycles: 1st heating up from 20 up to 300 °C at 10 °C/min, then cooling down up to 20 °C at −10 °C/min, and finally 2nd heating from 20 up to 300 °C at 10 °C/min. The glass transition temperature was evaluated on the 2nd heating curve.

The fire behavior of the prepared samples was deeply investigated through forced-combustion tests. In particular, a **cone calorimeter** (CC), as Noselab instrument (Nova Milanese, Italy), working with a 35
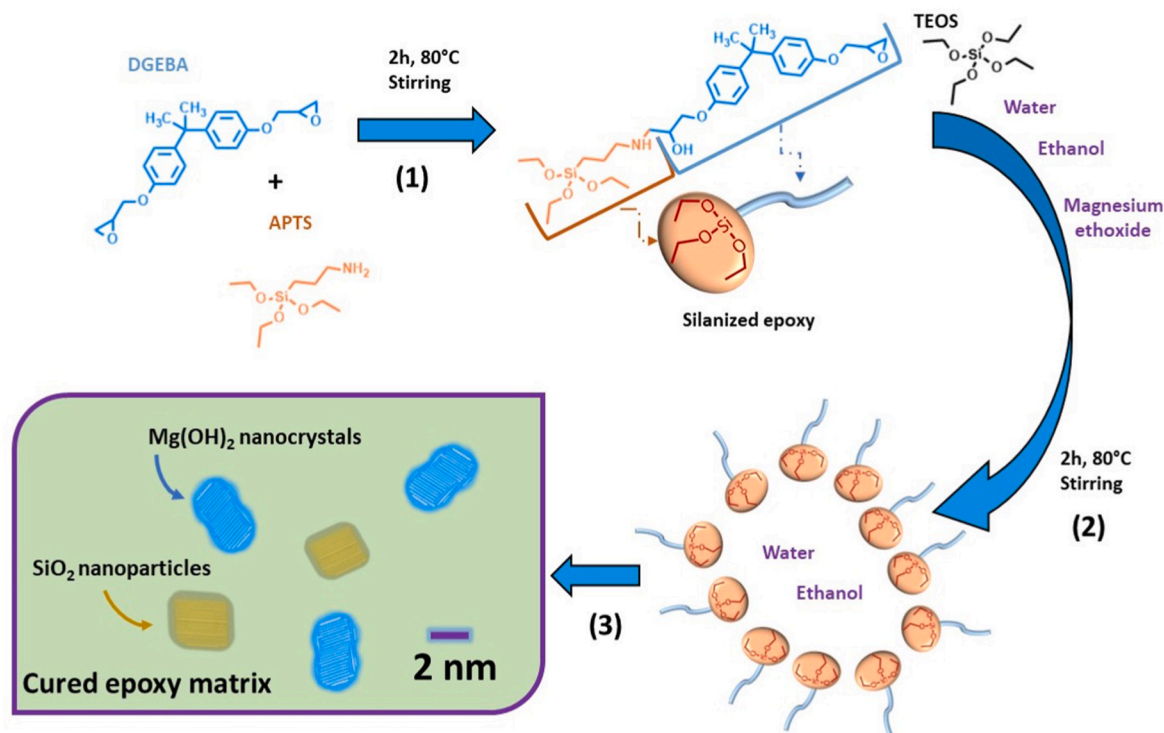
Fig. 1. Overall procedure for the synthesis of hybrid Mg(OH)$_2$–epoxy flame retardant nanocomposites. DGEBA: bisphenol A diglycidyl ether; APTS: 3-aminopropyl-triethoxysilane; TEOS: tetraethyl orthosilicate. On the left with blue and yellow colours, twinned Mg(OH)$_2$ nanocrystals with a pseudo-hexagonal morphology and a few multisheet-silica nanoparticles are represented, respectively. (For interpretation of the references to colour in this figure legend, the reader is referred to the Web version of this article.)

kW/m^2 irradiative heat flux and placing the samples (50 × 50 × 2 mm^3) in horizontal configuration was used, following the ISO 5660 standard. Several parameters (namely, time to ignition (TTI, s), peak of heat release rate (pHRR, kW/m^2), total heat release (THR, kW/m^2), total smoke release (TSR, m^2/m^2), specific extinction area (SEA, m^2/kg), and the residues) of samples were measured. With respect to pyrolysis combustion flow calorimetry, CC involves the use of a spark to trig the flaming combustion of volatiles generated by heat radiation, as required by the ISO 5660 standard. A **pyrolysis combustion flow calorimeter** (PCFC, Fire Testing Technology Instrument, London, UK), following the ASTM D7309 standard, was employed to assess pHRR, THR, and HRC. In the pyrolysis zone, samples of about 7 mg were heated from 150 to 750 °C at 1 K/s. Three tests were carried out on each material system and the results averaged.

2.4. Machine learning predictive analysis

KNIME version 4.0.2 (available free of charge at https://www.knime.com/download-previous-versions) was used as open-source software for creating data science. The estimation of the HRC of the in-situ hybrid Mg(OH)$_2$-epoxy nanocomposite (EPO-Mg) was performed by a supervised machine learning approach.

3. Results and discussion

3.1. Glass transition temperature of Epoxy/Mg(OH)$_2$ nanocomposite

The procedure leading to the formation of twinned Mg(OH)$_2$-based nanocrystals with a pseudo-hexagonal symmetry in the hybrid epoxy-silane matrix is summarized in Fig. 1. Fig. S1 shows that the in-situ generation of Mg(OH)$_2$ nanocrystals leads to a glass transition temperature of 82 °C, a lower value (~14%) compared to that of the unmodified epoxy resin. This finding may be due to the presence of crystalline domains (Fig. 1) which negatively affect the polymer chains, owing to their disturbance during the establishment of inter-chain interactions in the curing process [35,36]. The higher glass transition of EPO with respect to EPO-Mg may be also ascribed to more dangling segments in the structure of the hybrid nanocomposite, resulting in a slight network loosening effect [36,37].

3.2. Fire behavior of the in-situ hybrid Mg(OH)$_2$-Epoxy nanocomposites

HRR curves for the epoxy system and its hybrid counterpart, obtained by cone calorimetry using a 35 kW/m^2 irradiative heat flux, together with fire and smoke parameters, are reported in Fig. 2a, Table 1 and Table 2, respectively. First of all, it is worth noting that the nano-filler is responsible for an anticipation of the TTI by about 15 s (Table 1). This finding is attributed to two main effects, i.e.: (i) the low amount (~5 wt%) of magnesium hydroxide nanocrystals, which is not enough to exert an effective thermal protection during the first combustion stages, and (ii) the basic character of Mg(OH)$_2$ that speeds up the kinetics of the pyrolysis reaction occurring under the exposure to the irradiative heat flux [7,11,38,39]. Besides, the presence of the nanofiller significantly improves some of the thermal and smoke parameters (Table 2), notwithstanding that its concentration is very low (i.e. 5 wt%, see section 2.2). The residue of the hybrid system at the end of the cone tests is almost doubled as compared to the pristine epoxy (Table 1 and Fig. 3), hence indicating that the ceramization effect induced by Mg(OH)$_2$ is very effective in protecting the underlying polymer network from the irradiative heat flux, slowing down the heat and mass transfer from the surroundings to the sample and vice versa. In particular, compared to pristine EPO, THR, pHRR, and HRR decrease by about 10, 37, and 29%, respectively, when the nanofiller is in-situ formed in the epoxy system (Fig. 2a and Table 1). Similarly, TSR and SEA values show a decrease of about 22 and 5% (Table 2), respectively, hence indicating that the nanofiller is quite effective as smoke suppressant, despite its very low
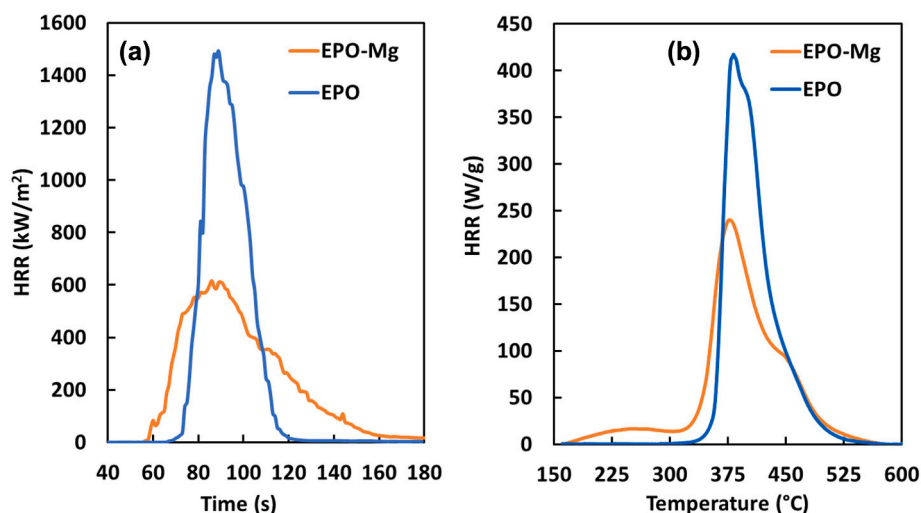
Fig. 2. Heat release rate (HRR) curves of samples measured using (a) cone calorimeter and (b) pyrolysis combustion flow calorimetry (PCFC).

Table 1

Results from cone calorimetry tests for unfilled epoxy and its hybrid nanocomposite.

Sample	TTI (s)	THR (MJ/m²)	ΔTHR (%)	pHRR (kW/m²)	ΔpHRR (%)	HRR (kW/m²)	ΔHRR (%)	FRI (−)	Residue (%)
EPO	46 ± 4	68 ± 3	–	1250 ± 54	–	292 ± 11	–	–	3 ± 0.4
EPO-Mg	31 ± 8	61 ± 7	−10.2	789 ± 47	−36.9	207 ± 14	−29.1	1.2	7 ± 0.2

Table 2

Smoke parameters from cone calorimetry tests for unfilled epoxy and its hybrid nanocomposite.

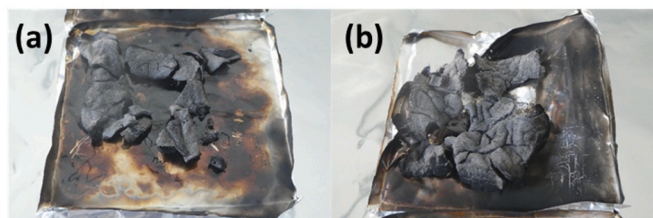| Sample	TSR (m²/ m²)	ΔTSR (%)	SEA (m²/ kg)	ΔSEA (%)	CO yield (kg/kg)	CO₂ yield (kg/kg)	CO/ CO₂
EPO	2500	–	938	–	$8 \bullet 10^{-3}$ $\pm$ $9 \bullet 10^{-3}$	$2 \bullet 10^{-2}$ $\pm$ $2 \bullet 10^{-2}$	0.33
EPO-Mg	1956	−21.7	887	−5.4	$5 \bullet 10^{-4}$ $\pm$ $1 \bullet 10^{-4}$	$5 \bullet 10^{-3}$ $\pm$ $6 \bullet 10^{-4}$	0.09

Fig. 3. Photographs of the char residues obtained after cone calorimetry tests for (a) EPO and (b) its hybrid nanocomposite (EPO-Mg).

loading in the epoxy system. Finally, CO/CO_2 ratio remarkably decreases (Table 2) in the presence of $Mg(OH)_2$, hence indicating a certain efficiency of combustion that does not inhibit the conversion of CO to CO_2 [11–13]. As a consequence, it can be argued that the flame retardant action of the nanofiller is more pronounced in the condensed phase, rather than in the gas phase. Flame retardancy index (FRI) is a dimensionless parameter that has been extensively used to compare the fire performances of flame retardant polymer-based systems with the ones of their unmodified counterparts [40–42]. Thanks to FRI, it is possible to rank the material and evaluate its fire response. As reported in Table 1, the FRI value (1.2) of EPO-Mg is very low and only allows for a

classification of the material as "poor". However, this result agrees with what was observed for in-situ silica-epoxy systems [3,43], for which a condensed phase action was also the main flame retardant mechanism. Based on that, the chemical composition of EPO-Mg could be modified by the addition of phosphorus (P)-based flame retardants and other synergists. This may significantly improve the fire response of EPO-Mg, resulting in an increase of FRI value. Besides, the incorporation of P-based compounds and nitrogen-containing species (e.g., melamine) may also positively affect the glass transition temperature of the nano-composite through the establishment of proper interactions in the polymer network, as already observed in a previous study [44,45].

Table 3 and Fig. 2b show the results of Pyrolysis Combustion Flow Calorimetry (PCFC) tests. PCFC apparatus allows for the evaluation of different parameters concerning the fire behavior of composites [46,47]. With respect to the cone calorimeter, the PCFC does not simulate a real fire scenario, as the combustion of the investigated samples is not performed in presence of air and does not involve the use of a spark ignition for the flame and a heat radiation source. PCFC is a non-flaming test, where the flaming combustion takes place in two separate chambers [46]. Indeed, PCFC measurements involve a controlled pyrolysis of the samples followed by the oxidation of the volatile products. This configuration makes the PCFC very helpful to better study the gas phase action of flame retardants [46,48,49]. The results provided by PCFC measurements additionally confirm the flame retardant action exerted by magnesium hydroxide in the condensed phase during the combustion. Similar to other metal hydroxides, magnesium hydroxide can reduce the heat transfer to the polymer bulk by a heat-sink effect, as its endothermic decomposition produces refractive oxide and water. The oxide acts as a thermal shield, in cooperation with the silica

Table 3

Results from pyrolysis combustion flow calorimeter for unfilled epoxy and its hybrid nanocomposite.

Sample	THR (kJ/g)	HRC (J/g-K)	pHRR (W/g)	Residue (%)
EPO	26 ± 5	427 ± 11	425 ± 10	5 ± 0.2
EPO-Mg	23 ± 2	281 ± 12	236 ± 13	9 ± 0.5

nanostructures, while the water dilutes the concentration of the flammable gases in the gas phase [3,50]. The thermal shield not only lowers the heat exchange but also the transfer of flammable gases and oxygen at the boundary phase during the combustion. The combination of all these effects results in the remarkable decrease of THR, HRC, and pHRR values of the nanocomposite with respect to pristine EPO (Table 3 and Fig. 2b). The protection of the ceramic shield leads to a notable increase in the residue at the end of PCFC (Table 3), which agrees with the cone calorimetry results. Some additional aspects are important to be mentioned, which further explain the lower values of THR, HRC, and pHRR measured by PCFC tests. Fig. 2b shows that the HRR curve of EPO is narrow, owing to a large amount of heat released in a short time. On the other side, the HRR curve of EPO-Mg appears flattened and broad, due to the strong condensed phase action of Mg(OH)$_2$ nanocrystals from the first decomposition steps, leading to a slow heat release over a longer period of time [51].

3.3. Prediction of the heat release capacity of in-situ hybrid Mg(OH)$_2$-Epoxy nanocomposites by machine learning

Machine learning techniques allow for the formulation of complex algorithms to describe a phenomenon that is not possible to model through a traditional approach. The human being learns rules of general validity from nature and usually, this learning occurs through an iterative process, which slowly increases our knowledge. Taking inspiration from this process, machine learning is a learning algorithm, as it provides specific operations to the machine that this latter will use to afford future experiences. The machine learns by data sets, which are inserted in a generic algorithm programmed to perform a particular function. Artificial neural networks (ANNs) consist of a set of algorithms for classification and regression, which have been widely used to solve different problems [52,53]. As the biological brain, neural networks are based on large groups of neurons connected by axons. The artificial neurons form an interconnected network of individual neural units. The connection between units can be reinforced or inhibited through a combination of the input values and an activation function, which returns the output of the neuron [19,54].

ANNs are mainly nonlinear mathematical functions able to transform a set of independent variables $x = (x_1, …, x_n)$, i.e., network inputs, into dependent variables $y = (y_1, …, y_k)$, i.e., network outputs. The obtained results depend on a set of values $w = (w_1, …, w_n)$, which are called weights. Eq. (1) represents the relationship between outputs and inputs of the network:

$$y = f \left(\sum_j w_j * x_j + b \right) \quad (1)$$

where:

- x_j is the jth input
- w_j is the jth weight
- b is the bias
- y is the output
- f is the activation function

During the training phase, the neuron recovers the information that will be located in the weights and biases and used in congruent situations. The activation function, f, is generally a threshold function that activates only neurons showing signals compatible with the threshold, hence the signal is transferred to the next neuron or neurons. Sigmoid, nonlinear stepped or logistic functions are some examples of activation functions [55]. An iterative procedure is responsible for adjusting the weights during the training phase. This procedure is computational-demanding and requires a certain number of input-target pairs, which are called training sets. Indeed, in training, the values of weights that minimize a specific error function are searched [56]. An

ANN is usually composed of three parts, containing distinct quantities of neurons: (i) an input level, (ii) several hidden levels, (iii) an output level. Through the neurons belonging to the internal layers, the input signals move from the input level to the output level, as displayed in Fig. 4.

The heat release capacity (HRC) depends on the fire behaviour and the thermal stability of a specific material, revealing its attitude to degrade under combustion. HRC can be used to classify the flammability of materials and can be evaluated from PCFC results (see section 3.1) or from additive molar group contributions [15]. As an alternative to these methodologies, some recent research works in the literature have demonstrated that artificial neural network (ANN) models represent a valuable approach for the prediction of HRC of several materials [27, 57]. ANN models can be very useful in case the PCFC apparatus is not available or low processing times (i.e., a reduced number of measurements) are required to investigate the combustion properties of a specific material. Herein, by the use of KNIME, an open-source software for creating data science and a supervised machine learning approach [58], we developed an artificial neural network-based model to predict the HRC value of EPO-Mg from its PCFC parameters and chemical-physical properties (input data set, Table S1). The input parameters for the model (columns of Table S1) consist of chemical-physical properties, HRC, THR, and char yield of several polymers, including EPO and EPO-Mg, whose experimental values were found in the literature [26]. A statistical analysis was performed on input dataset to estimate mean and variance of each different parameter. The results of this analysis, collected in Table S2, clearly show the heterogeneity among the selected classes of polymers. The physico-chemical properties of EPO and EPO-Mg were assumed the same and equal to those of an epoxy resin cured with an aliphatic amine hardener (i.e., EPA in Ref. [26]). For the hybrid Mg(OH)$_2$-epoxy nanocomposite (EPO-Mg) and the pristine resin (EPO), the values of Tg, HRC, THR, and char yield were experimentally measured in this research work by DSC and PCFC tests, respectively. As shown in section 3.1, the HRC value of EPO-Mg gathered from PCFC measurements was found around 281 J/g-K and will be used, together with the HRC values of the other polymers (Table S1), to evaluate the reliability of the developed ANN model through a sensitivity analysis. The validation of the artificial neural network-based system relies on the verification of the predictive capacity of the model exploiting never used input data. To avoid an overfitting for the model, the number of input parameters was chosen considering the number of available observations.

We split the input data set into two subsets: the training set and the test set. The training set (Table S3) was employed for training the model, while the test set (Table S4) for evaluating the model's forecasting capability. A measure of the model's performance was carried out by
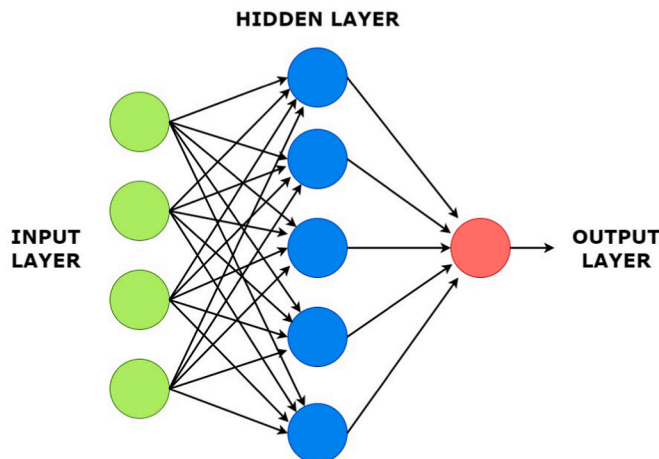

Fig. 4. Schematic representation of a generic artificial neural network with nodes-related weighted connections.

assessing the accuracy of the test data. The input data (Table S1) set was randomly split as follows: 70% of training data set and 30% of test data set. The connection weights based on the error committed on the output production are adjusted by the training data set that contains 34 observations. On the other side, the test data set (Table S4), containing 15 observations, represents instances available for the test and can be used to validate the algorithm and verify the network's forecasting capacity, when it receives input data never seen before (HRC column in Table S3), which will be named as "new data" in the following.

The simulation model developed in this research work is a fully connected feed-forward artificial neural network based on a multilayer perceptron [59,60]. Fig. 5 shows the architecture of the model based on neural networks and the structure of each layer. The structure mainly consists of an input layer with twelve variables (molecular weight, M_w; Van-der-Waals volume, $V_{van-der-Waals}$; molar volume, V_m; density, ρ; solubility parameter, δ_p; molar cohesive energy, e_{coh}; glass transition temperature, T_g; molar heat capacity, C_n; index of refraction and entanglement, N; entanglement molecular weight, M_w; THR and char yield from PCFC measurements), as shown in Table S1, one hidden layer with six neurons and an output layer with a single neuron that returns the predicted heat release capacity of the material.

To predict the values of HRC for EPO-Mg, our artificial neural model performs a locally weighted regression with the use of a trained multilayer perceptron classifier, which performs the regression, and a k-nearest neighbors algorithm (K-NN) [61]. We employed this supervised machine learning algorithm to assign weights to the training data, considering their distance from the new data. The assigned weight for each training data point is inversely proportional to its distance from the new data point (Fig. 6). Thus, when the classifier performs the regression, it gives more consideration to "local" data (i.e., the training data in the K-regions, which are the nearest data to the new ones), leading to more accurate results compared with a normal regression approach.

Generally speaking, the training of a multilayer perceptron model involves two main steps: (i) the tuning of the hyperparameters and (ii) the validation of the model trained with the hyperparameters by using a subset of the input data [62,63]. In addition to these steps, to obtain a more accurate prediction of the test data set and thus also of the HRC
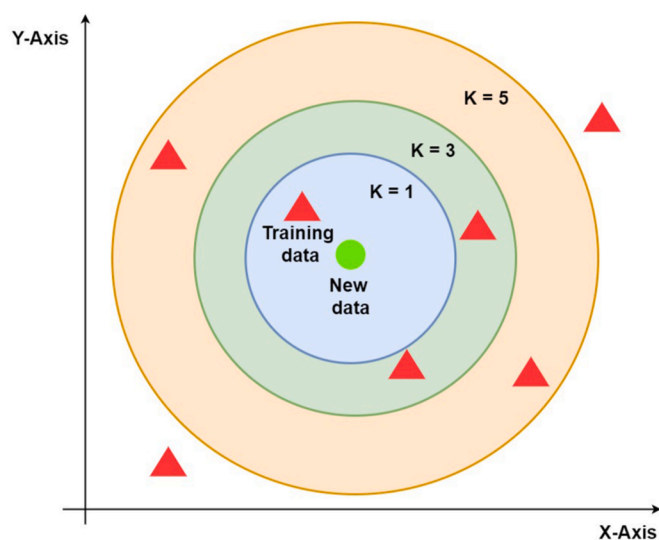

Fig. 6. Operating principles of a K-NN algorithm. Red triangles represent the nearest training data to the new data (green circle) or "never seen before" input data. These training data are called "local data" and are confined in specific K-regions. (For interpretation of the references to colour in this figure legend, the reader is referred to the Web version of this article.)

value of EPO-Mg, we performed the "cleaning" of the input data for the algorithm. This data cleaning phase involves two pre-processing procedures consisting of correlation filtering and Z-Score normalization. The correlation allows for a reduction of the redundant columns of input data of Table 1, which do not provide useful or necessary information for the algorithm and its accuracy. The correlation threshold was chosen as 70%: therefore, all the columns with a correlation value greater than this were not considered as input data set for our model. Subsequently, the Z-Score normalization of the input data of Table 1 was also carried out by applying Eq. (2):
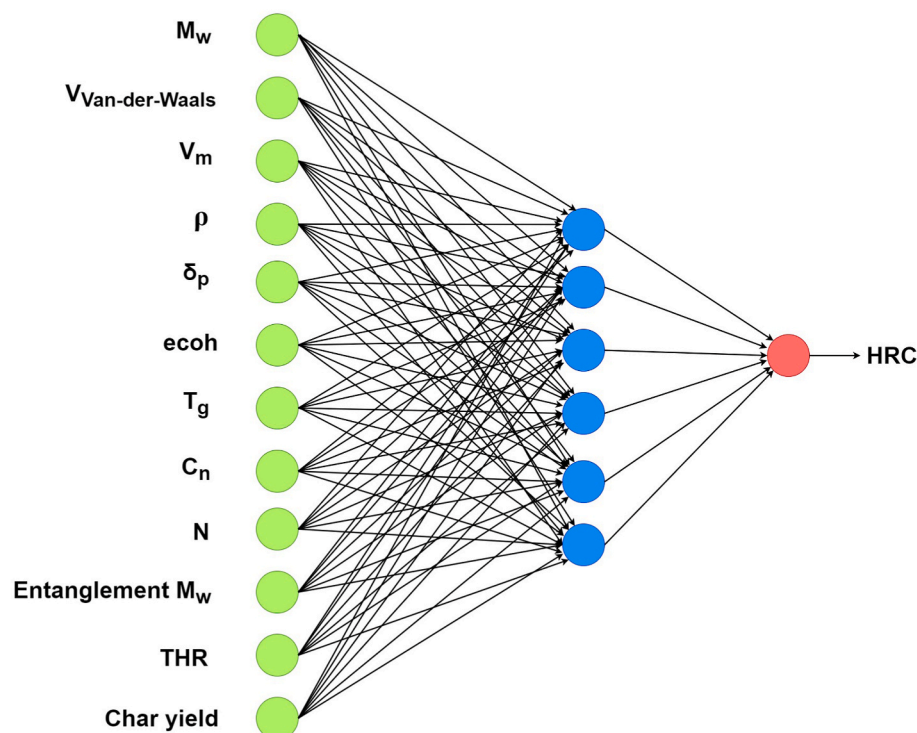
Fig. 5. Artificial neural network model architecture composed by three layers. M_w, molecular weight (g/mol); $V_{van-der-Waals}$, Van-der-Waals volume (mL/mol), V_m is molar volume (mL/mol), ρ is density (g/mL), δ_p is solubility parameter (MPa$^{1/2}$), ecoh is molar cohesive energy (J/mol), T_g is glass transition temperature (K), C_n is molar heat capacity (J/mol-K), N is the index of refraction and entanglement, M_w is the entanglement molecular weight (g/mol), THR is the total heat release (kJ/g), HRC is the heat release capacity (J/g-K).

$$Z = \frac{x - \mu}{\sigma} \tag{2}$$

where:

- Z is the final normalized value
- x is the original value
- μ is the average value
- σ is the standard deviation

The Z-Score normalization is very useful to handle outliers and has been shown in the literature to increase the accuracy of regression models [64]. After the cleaning process, the input data set appears as reported in Table S5, which is reduced to eight columns showing values of M_w, $V_{van-der-Waals}$, δ_p, T_g, N, M_w entanglement molecular weight, THR and char yield for the remaining polymers. Normalized input data set was used to predict the HRC value of the EPO-Mg.

After the cleaning process, we performed a tuning phase mainly concerning the search of the values of the hyperparameters able to minimize both the root mean square error (RMSE) and the mean absolute error (MAE) for the algorithm [65,66]. The minimization of both errors involved the use of a "Parameter Optimization Loop (POL)". In the present research study, POL was exploited for finding the best combination of hyperparameters (such as the "K" parameter of K-NN algorithm and the internal hyperparameters of the ANN), which minimize the global error when performing locally weighted regressions on each subset of the input data (extracted through the "X-Partitioner" node) [22]. As mentioned, two types of hyperparameters were tuned: "K" (i.e., number of neighbors), which belongs to the K-NN algorithm, and the internal hyperparameters (e.g., the learning rate, the momentum, and the number of epochs) of the multilayer perceptron [67]. K equal to 9 was found as the best value for our K-NN algorithm, as it gives the lowest RMSE and MAE. After this tuning phase, the HRC values for the test data set were predicted (Table S4) and the values of RMSE and MAE were evaluated at around 145.6 and 186.1, respectively. MAE and RMSE provide an insight into the average distance between the experimental values and the ones predicted by the model [65,66]. These values of MAE and RMSE confirm that our algorithm has a good predictive capability, as the predicted HRC values are very close to the experimental ones. The trained algorithm provides a predicted value of HRC for EPO-Mg of around 273 J/g-K (Table S6), which is quite similar to the experimental value (281 J/g-K), in the range of discrepancy (Table 3). The whole KNIME workflow employed in this research work to predict the HRC value is reported in Fig. S2.

4. Conclusions

In this work, we evaluated the fire behavior of an hybrid $Mg(OH)_2$-epoxy nanocomposite and correlated the experimental data to modeling its heat release capacity. The epoxy nanocomposite exhibited lower glass transition temperature compared to the unmodified resin, probably due to the presence of nanocrystals resulting in some disturbing effects during the establishment of inter-chain interactions. Interestingly, despite the very low loading (~5 wt%) of the in-situ generated nanofiller, $Mg(OH)_2$ nanocrystals were able to significantly lower the fire and smoke parameters during cone calorimetry and pyrolysis combustion flow calorimetry tests, hence enhancing the overall flame retardant behavior of the epoxy network. Then, a machine learning approach was designed for building a model, based on simple data (i.e., training data), able to make predictions without being explicitly programmed to perform that function. In particular, the developed artificial neural network-based system was able to effectively predict the heat release capacity of the prepared $Mg(OH)_2$-epoxy nanocomposite, resulting in low error values (MAE and RMSE equal to 145.6 and 186.1, respectively). This research demonstrates that machine learning may be considered a valuable tool for predicting the fire performances of novel flame retardant polymer-based nanocomposites and better designing their future functionalities.

CRediT author statement

Aurelio Bifulco and **Angelo Casciello**: Conceptualization, Methodology, Formal analysis, Investigation, Validation, Writing - Original Draft. **Giulio Malucelli**: Conceptualization, Methodology, Supervision, Resources, Writing - Review and Editing. **Sabyasachi Gaan** and **Stanislao Forte**: Resources, Writing - Review and Editing. **Antonio Aronne** and **Claudio Imparato**: Methodology, Validation, Writing - Review and Editing. All authors commented on the final manuscript of this study.

Declaration of competing interest

The authors declare the following financial interests/personal relationships which may be considered as potential competing interests:
Aurelio Bifulco reports financial support was provided by Italian Ministry of Education and Research. Aurelio Bifulco reports a relationship with University of Naples Federico II that includes: employment.

Data availability

Data will be made available on request.

Acknowledgements

Appendix A. Supplementary data

Supplementary data to this article can be found online at https://doi.org/10.1016/j.polymertesting.2023.108175.

References

[1] L. Guadagno, M. Raimondo, V. Vittoria, L. Vertuccio, C. Naddeo, S. Russo, B. De Vivo, P. Lamberti, G. Spinelli, V. Tucci, Development of epoxy mixtures for application in aeronautics and aerospace, RSC Adv. 4 (2014) 15474–15488.

[2] X.-F. Liu, B.-W. Liu, X. Luo, D.-M. Guo, H.-Y. Zhong, L. Chen, Y.-Z. Wang, A novel phosphorus-containing semi-aromatic polyester toward flame retardancy and enhanced mechanical properties of epoxy resin, Chem. Eng. J. 380 (2019), 122471-122471.

[3] A. Bifulco, C. Imparato, A. Aronne, G. Malucelli, Flame retarded polymer systems based on the sol-gel approach: recent advances and future perspectives, J. Sol. Gel Sci. Technol. (2022) 1–25.

[4] M. Ciesielski, J. Diederichs, M. Döring, A. Schäfer, Advanced Flame-Retardant Epoxy Resins for Composite Materials, Fire and Polymers V, American Chemical Society, 2009, pp. 174–190.

[5] Y.-F. Ai, F.-Q. Pang, Y.-L. Xu, R.-K. Jian, Multifunctional phosphorus-containing triazolyl amine toward self-intumescent flame-retardant and mechanically strong epoxy resin with high transparency, Ind. Eng. Chem. Res. 59 (2020) 11918–11929.

[6] Y. Liu, Y. Gao, Q. Wang, W. Lin, The synergistic effect of layered double hydroxides with other flame retardant additives for polymer nanocomposites: a critical review, Dalton Trans. 47 (2018) 14827–14840.

[7] M. Martins, C. Pereira, A study on the effect of nano-magnesium hydroxide on the flammability of epoxy resins, Solid State Phenom. 151 (2009) 72–78.

[8] J. Xiao, J. Hobson, A. Ghosh, M. Haranczyk, D.-Y. Wang, Flame retardant properties of metal hydroxide-based polymer composites: a machine learning approach, Compos. Commun. 40 (2023), 101593.

[9] Y.-Y. Yen, H.-T. Wang, W.-J. Guo, Synergistic flame retardant effect of metal hydroxide and nanoclay in EVA composites, Polym. Degrad. Stabil. 97 (2012) 863–869.

[10] T. Zhang, W. Liu, M. Wang, P. Liu, Y. Pan, D. Liu, Synergistic effect of an aromatic boronic acid derivative and magnesium hydroxide on the flame retardancy of epoxy resin, Polym. Degrad. Stabil. 130 (2016) 257–263.

[11] R. Suihkonen, K. Nevalainen, O. Orell, M. Honkanen, L. Tang, H. Zhang, Z. Zhang, J. Vuorinen, Performance of epoxy filled with nano-and micro-sized magnesium hydroxide, J. Mater. Sci. 47 (2012) 1480–1488.

[12] N. Li, Z. Li, Z. Liu, Y. Yang, Y. Jia, J. Li, M. Wei, L. Li, D.y. Wang, Magnesium hydroxide micro-whiskers as super-reinforcer to improve fire retardancy and mechanical property of epoxy resin, Polym. Compos. 43 (2022) 1996–2009.

[13] F. Branda, J. Passaro, R. Pauer, S. Gaan, A. Bifulco, Solvent-free one-pot synthesis of epoxy nanocomposites containing Mg(OH)2 nanocrystal–nanoparticle formation mechanism, Langmuir 38 (2022) 5795–5802.

[14] A. Bifulco, F. Tescione, A. Capasso, P. Mazzei, A. Piccolo, M. Durante, M. Lavorgna, G. Malucelli, F. Branda, Effects of post cure treatment in the glass transformation range on the structure and fire behavior of in situ generated silica/epoxy hybrids, J. Sol. Gel Sci. Technol. 87 (2018) 156–169.

[15] R.N. Walters, R.E. Lyon, Molar group contributions to polymer flammability, J. Appl. Polym. Sci. 87 (2003) 548–563.

[16] R. Sonnier, B. Otazaghine, F. Iftene, C. Negrell, G. David, B.A. Howell, Predicting the flammability of polymers from their chemical structure: an improved model based on group contributions, Polymer 86 (2016) 42–55.

[17] R. Sonnier, B. Otazaghine, L. Dumazert, R. Menard, A. Viretto, L. Dumas, L. Bonnaud, P. Dubois, N. Safronava, R. Walters, Prediction of thermosets flammability using a model based on group contributions, Polymer 127 (2017) 203–213.

[18] R.E. Lyon, M.T. Takemori, N. Safronava, S.I. Stoliarov, R.N. Walters, A molecular basis for polymer flammability, Polymer 50 (2009) 2608–2617.

[19] G. Ciaburro, G. Iannace, J. Passaro, A. Bifulco, A.D. Marano, M. Guida, F. Marulo, F. Branda, Artificial neural network-based models for predicting the sound absorption coefficient of electrospun poly (vinyl pyrrolidone)/silica composite, Appl. Acoust. 169 (2020), 107472.

[20] K. Guo, Z. Yang, C.-H. Yu, M.J. Buehler, Artificial intelligence and machine learning in design of mechanical materials, Mater. Horiz. 8 (2021) 1153–1172.

[21] S. Ye, B. Li, H.-P. Zhao, X.-Q. Feng, Deep neural network method for predicting the mechanical properties of composites, Appl. Phys. Lett. 115 (2019), 161901.

[22] H.J.P. Weerts, A.C. Mueller, J. Vanschoren, Importance of Tuning Hyperparameters of Machine Learning Algorithms, 2020 arXiv preprint arXiv: 2007.07588.

[23] C.A. Micchelli, M. Pontil, P. Bartlett, Learning the kernel function via regularization, J. Mach. Learn. Res. 6 (2005).

[24] W.S. Cleveland, S.J. Devlin, Locally weighted regression: an approach to regression analysis by local fitting, J. Am. Stat. Assoc. 83 (1988) 596–610.

[25] H. Vahabi, M.Z. Naser, M.R. Saeb, Fire protection and materials flammability control by artificial intelligence, Fire Technol. 58 (2022) 1071–1073.

[26] L. Jiang, R.A. Mensah, S. Asante-Okyere, M. Försth, Q. Xu, Y.Y. Ziggah, Á. Restás, F. Berto, O. Das, Developing an artificial intelligent model for predicting combustion and flammability properties, Fire Mater. 46 (2022) 830–842.

[27] Á. Pomázi, A. Toldy, Predicting the flammability of epoxy resins from their structure and small-scale test results using an artificial neural network model, J. Therm. Anal. Calorim. 148 (2023) 243–256.

[28] H. Jabbar, R.Z. Khan, Methods to avoid over-fitting and under-fitting in supervised machine learning (comparative study), Comput. Sci. Commun. Instrum. Dev. 70 (2015) 978–981.

[29] P.V. Parandekar, A.R. Browning, O. Prakash, Modeling the flammability characteristics of polymers using quantitative structure–property relationships (QSPR), Polym. Eng. Sci. 55 (2015) 1553–1559.

[30] S. Asante-Okyere, Q. Xu, R.A. Mensah, C. Jin, Y.Y. Ziggah, Generalized regression and feed forward back propagation neural networks in modelling flammability characteristics of polymethyl methacrylate (PMMA), Thermochim. Acta 667 (2018) 79–92.

[31] R.A. Mensah, L. Jiang, S. Asante-Okyere, Q. Xu, C. Jin, Comparative evaluation of the predictability of neural network methods on the flammability characteristics of extruded polystyrene from microscale combustion calorimetry, J. Therm. Anal. Calorim. 138 (2019) 3055–3064.

[32] J. Jiao, P. Liu, L. Wang, Y. Cai, One-step synthesis of improved silica/epoxy nanocomposites with inorganic-organic hybrid network, J. Polym. Res. 20 (2013), 202-202.

[33] F. Branda, A. Bifulco, D. Jehnichen, D. Parida, R. Pauer, J. Passaro, S. Gaan, D. Pospiech, M. Durante, Structure and bottom-up formation mechanism of multisheet silica-based nanoparticles formed in an epoxy matrix through an in situ process, Langmuir 37 (2021) 8886–8893.

[34] F. Branda, D. Parida, R. Pauer, M. Durante, S. Gaan, G. Malucelli, A. Bifulco, Effect of the coupling agent (3-aminopropyl) triethoxysilane on the structure and fire behavior of solvent-free one-pot synthesized silica-epoxy nanocomposites, Polymers 14 (2022) 3853.

[35] G. Luciani, A. Costantini, B. Silvestri, F. Tescione, F. Branda, A. Pezzella, Synthesis, structure and bioactivity of pHEMA/SiO 2 hybrids derived through in situ sol–gel process, J. Sol. Gel Sci. Technol. 46 (2008) 166–175.

[36] A. Bifulco, R. Avolio, S. Lehner, M.E. Errico, N.J. Clayden, R. Pauer, S. Gaan, G. Malucelli, A. Aronne, C. Imparato, In Situ P-Modified Hybrid Silica–Epoxy Nanocomposites via a Green Hydrolytic Sol–Gel Route for Flame-Retardant Applications, ACS Applied Nano Materials, 2023.

[37] F. Wang, S. Pan, P. Zhang, H. Fan, Y. Chen, J. Yan, Synthesis and application of phosphorus-containing flame retardant plasticizer for polyvinyl chloride, Fibers Polym. 19 (2018) 1057–1063.

[38] G. Grause, K. Sugawara, T. Mizoguchi, T. Yoshioka, Pyrolytic hydrolysis of polycarbonate in the presence of earth-alkali oxides and hydroxides, Polym. Degrad. Stabil. 94 (2009) 1119–1124.

[39] A.A. Pilarska, Ł. Klapiszewski, T. Jesionowski, Recent development in the synthesis, modification and application of Mg (OH) 2 and MgO: a review, Powder Technol. 319 (2017) 373–407.

[40] H. Vahabi, B.K. Kandola, M.R. Saeb, Flame retardancy index for thermoplastic composites, Polymers 11 (2019) 407.

[41] E. Movahedifar, H. Vahabi, M.R. Saeb, S. Thomas, Flame retardant epoxy composites on the road of innovation: an analysis with flame retardancy index for future development, Molecules 24 (2019) 3964.

[42] H. Vahabi, E. Movahedifar, B.K. Kandola, M.R. Saeb, Flame Retardancy Index (FRI) for polymer materials ranking, Polymers 15 (2023) 2422.

[43] A. Bifulco, D. Parida, K.A. Salmeia, R. Nazir, S. Lehner, R. Stämpfli, H. Markus, G. Malucelli, F. Branda, S. Gaan, Fire and mechanical properties of DGEBA-based epoxy resin cured with a cycloaliphatic hardener: combined action of silica, melamine and DOPO-derivative, Mater Design 193 (2020), 108862-108862.

[44] V. Venezia, S. Matta, S. Lehner, G. Vitiello, A. Costantini, S. Gaan, G. Malucelli, F. Branda, G. Luciani, A. Bifulco, Detailed thermal, fire, and mechanical study of silicon-modified epoxy resin containing humic acid and other additives, ACS Appl. Polym. Mater. 3 (2021) 5969–5981.

[45] A. Bifulco, D. Parida, K. Salmeia, S. Lehner, R. Stämpfli, H. Markus, G. Malucelli, F. Branda, S. Gaan, Improving flame retardancy of in-situ silica-epoxy nanocomposites cured with aliphatic hardener: combined effect of DOPO-based flame-retardant and melamine, Composites Part C: Open Access 2 (2020).

[46] R.E. Lyon, R.N. Walters, Pyrolysis combustion flow calorimetry, J. Anal. Appl. Pyrol. 71 (2004) 27–46.

[47] Z.-S. Li, J.-G. Liu, T. Song, D.-X. Shen, S.-Y. Yang, Synthesis and characterization of novel phosphorous-silicone-nitrogen flame retardant and evaluation of its flame retardancy for epoxy thermosets, J. Appl. Polym. Sci. 131 (2014), 40412/40411-40412/40410.

[48] S. Molyneux, A.A. Stec, T.R. Hull, The effect of gas phase flame retardants on fire effluent toxicity, Polym. Degrad. Stabil. 106 (2014) 36–46.

[49] Q. Xu, R.A. Mensah, C. Jin, L. Jiang, A critical review of the methods and applications of microscale combustion calorimetry for material flammability assessment, J. Therm. Anal. Calorim. (2021) 1–13.

[50] J. Green, Mechanisms for flame retardancy and smoke suppression-a review, J. Fire Sci. 14 (1996) 426–442.

[51] Q. Li, P. Jiang, Z. Su, P. Wei, G. Wang, X. Tang, Synergistic effect of phosphorus, nitrogen, and silicon on flame-retardant properties and char yield in polypropylene, J. Appl. Polym. Sci. 96 (2005) 854–860.

[52] T. Hill, L. Marquez, M. O'Connor, W. Remus, Artificial neural network models for forecasting and decision making, Int. J. Forecast. 10 (1994) 5–15.

[53] J. von Grabe, Potential of artificial neural networks to predict thermal sensation votes, Appl. Energy 161 (2016) 412–424.

[54] J. Liu, J. Sun, S. Wang, Pattern recognition: an overview, IJCSNS Int. J. Comput. Sci.Netw. Secur. 6 (2006) 57–61.

[55] S. Sharma, S. Sharma, A. Athaiya, Activation functions in neural networks, Data Sci. 6 (2017) 310–316.

[56] M. Cilimkovic, Neural Networks and Back Propagation Algorithm, Institute of Technology Blanchardstown, Blanchardstown Road North Dublin, 2015, p. 15.

[57] H.T. Nguyen, K.T.Q. Nguyen, T.C. Le, L. Soufeiani, A.P. Mouritz, Predicting heat release properties of flammable fiber-polymer laminates using artificial neural networks, Compos. Sci. Technol. 215 (2021), 109007.

[58] A. Fillbrunn, C. Dietz, J. Pfeuffer, R. Rahn, G.A. Landrum, M.R. Berthold, KNIME for reproducible cross-domain analysis of life science data, J. Biotechnol. 261 (2017) 149–156.

[59] H. Ramchoun, M.A.J. Idrissi, Y. Ghanou, M. Ettaouil, Multilayer Perceptron: architecture Optimization and training with mixed activation functions, in: Proceedings of the 2nd International Conference on Big Data, Cloud and Applications 71, 2017, pp. 1–6.

[60] H. Ramchoun, Y. Ghanou, M. Ettaouil, M.A. Janati Idrissi, Multilayer perceptron: architecture optimization and training, Int. J. Interact. Multimed. and Artif. Intell. 4 (2016) 26–30.

[61] O. Kramer, Dimensionality Reduction with Unsupervised Nearest Neighbors, Springer, 2013.

[62] R. Neuneier, H.G. Zimmermann, How to Train Neural Networks, Neural Networks: Tricks of the Trade, Springer, 2002, pp. 373–423.

[63] G. Zimmermann, R. Grothmann, C. Tietz, R. Neuneier, Market Modeling Based on Cognitive Agents, Springer, pp. 1061-1067.

[64] J.M. Cochran, A. Leproux, D.R. Busch, T.D. O'Sullivan, W. Yang, R.S. Mehta, A. M. Police, B.J. Tromberg, A.G. Yodh, Breast cancer differential diagnosis using diffuse optical spectroscopic imaging and regression with z-score normalized data, J. Biomed. Opt. 26 (2021), 026004-026004.

[65] J. Qi, J. Du, S.M. Siniscalchi, X. Ma, C.-H. Lee, On mean absolute error for deep neural network based vector-to-vector regression, IEEE Signal Process. Lett. 27 (2020) 1485–1489.

[66] A. Botchkarev, Performance Metrics (Error Measures) in Machine Learning Regression, Forecasting and Prognostics: Properties and Typology, arXiv Preprint arXiv:1809.03006, 2018.

[67] N.A. Hamid, N.M. Nawi, R. Ghazali, M.N.M. Salleh, M. Najib, Improvements of back propagation algorithm performance by adaptively changing gain, momentum and learning rate, Int. J. N. Comput. Archit. their Appl. 1 (2011) 866–878 (TOC).